Published in final edited form as:
Neurorehabil Neural Repair. 2012 January ; 26(1): . doi:10.1177/1545968311411054.

Upstream Dysfunction of Somatomotor Functional Connectivity after Corticospinal Damage in Stroke

Alex R. Carter, MD, PhD[1], **Kevin R. Patel, BA**[1], **Serguei V. Astafiev, PhD**[2], **Abraham Z. Snyder, PhD,MD**[1,2], **Jennifer Rengachary, MSOT**[1], **Michael J. Strube, PhD**[3,5], **Daniel L. W. Pope, BS**[2], **Joshua S. Shimony, MD**[2], **Catherine E. Lang, PhD**[1,3,4], **Gordon L. Shulman, PhD**[1], and **Maurizio Corbetta, MD**[1,2,6]

[1]Department of Neurology, Washington University School of Medicine, St. Louis, MO 63110, USA

[2]Malinckrodt Institute of Radiology, Washington University School of Medicine, St. Louis, MO 63110, USA

[3]Program in Physical Therapy, Washington University School of Medicine, St. Louis, MO 63108, USA

[4]Program in Occupational Therapy, Washington University School of Medicine, St. Louis, MO 63108, USA

[5]Department of Psychology, Washington University in St. Louis, St. Louis, MO 63130, USA

[6]Department of Anatomy and Neurobiology, Washington University School of Medicine, St. Louis, MO 63110, USA

Abstract

Background—Recent studies have shown that focal injuries can have remote effects on network function that impact behavior but these network-wide repercussions are poorly understood.

Objective—This study tested the hypothesis that lesions specifically to the outflow tract of a distributed network can result in upstream dysfunction in structurally intact portions of the network. In the somatomotor system this upstream dysfunction hypothesis predicted that lesions of the corticospinal tract might be associated with functional disruption within the system. Motor impairment might then reflect the dual contribution of corticospinal damage and altered network functional connectivity.

Methods—Twenty-three subacute stroke patients and thirteen healthy controls participated in the study. Corticospinal tract damage was quantified using a template of the tract generated from diffusion tensor imaging in healthy controls. Somatomotor network functional integrity was determined by resting state functional connectivity magnetic resonance imaging.

Author Contributions:
A.R.C. performed the analysis of most of the BOLD functional connectivity analysis and stroke lesion segmentation analysis, imaging-behavior correlations, and statistical analysis, assisted in the recruitment and scanning of subjects, and wrote the paper. K.P. performed most of the DTI analysis, developed the corticospinal tract template, and performed imaging-behavior correlations. S.V.A. assisted in the scanning of subjects, image analysis, ROI creation, and encoding of behavioral data, and developed the composite functional connectivity scores. A.Z.S. developed a new target atlas required for the DTI analysis and assisted K.P. in the DTI analysis. J.R. recruited and obtained consent from patients, assisted in the scanning, administered the behavioral battery, and analyzed the behavioral data. M.J.S. instructed the authors in statistical methods. J.S.S. assisted in the acquisition and analysis of DTI data. C.E.L. contributed to the experimental design and development of an appropriate battery for testing motor behavior. D.L.W.P. assisted in scanning, behavioral testing and image processing. G.L.S. and M.C. designed the study, oversaw data acquisition and analysis, and were principal editors of the paper. All authors discussed the results and/or commented on the paper.

Results—The extent of corticospinal damage was negatively correlated with inter-hemispheric resting functional connectivity, in particular with connectivity between the left and right central sulcus. While corticospinal damage accounted for much of the variance in motor performance, the behavioral impact of resting connectivity was greater in subjects with mild or moderate corticospinal damage, and less in those with severe corticospinal damage.

Conclusions—Our results demonstrated that dysfunction of cortical functional connectivity can occur after interruption of corticospinal outflow tracts, and can contribute to impaired motor performance. Recognition of these secondary effects from a focal lesion is essential for understanding brain-behavior relationships after injury, and may have important implications for neurorehabilitation.

Keywords

Motor performance; resting state functional connectivity/rsFC; stroke; corticospinal tract/CST; functional MRI/fMRI; diffusion tensor imaging/DTI

INTRODUCTION

Traditional localization theories in neurology emphasize the relationship between focal structural damage and behavioral deficits. However, recent advances in computational neuroscience[1-3] have indicated that brain networks are widely distributed.[4,5] Accordingly, many neuroimaging studies have reported abnormalities in task-evoked blood oxygen level dependent (BOLD) activity after injury in structurally intact regions. Furthermore, recovery of behavioral deficits has been associated with normalization of activity in the damaged hemisphere and with rebalancing of activity across hemispheres[6-13]. More recently, changes in functional connectivity (FC), i.e. the inter-regional correlation of task-evoked or spontaneous activity, have also been documented after stroke and associated with neurological deficits.[14-17] These observations raise a fundamental question: what is the relationship between structural damage and physiologic abnormalities in regions that are distant from the area of damage?[1,18,19] Here, we considered how resting state functional connectivity (rsFC) in the somatomotor network is influenced by structural damage to its major outflow, the corticospinal tract (CST), where the somatomotor network is operationally defined as the regions showing significant functional connectivity with the primary somatomotor cortex (central sulcus).[20] The human somatomotor network is a good system in which to explore our question because much is already known about its components and connections[21-24] and how CST damage impacts motor recovery.[25-27]

We studied whether rsFC in the somatomotor network was influenced by the degree of structural damage to the CST in 23 patients with subacute stroke. Assuming that somatomotor rsFC depends predominantly on the integrity of reciprocal cortico-cortical or cortico-thalamic connections,[15, 28, 29] one possibility was that CST damage would not correlate with changes in rsFC. Alternatively, any correlation between rsFC and CST damage would imply that the spontaneous coherence of motor regions changes in response to CST injury. The mechanisms underlying such a relationship are not known but could involve compensatory cortical over-activation,[30, 31] activity dependent plasticity,[32-34] and structural remodeling of pyramidal cells in cortical layer V.[35] We also investigated the relative contributions of CST damage and somatomotor rsFC to motor deficits.

To investigate the relationship between CST damage and rsFC, a correlational approach was used. To determine the separate contributions of CST damage and rsFC to behavioral impairment and the presence of any rsFC × CST damage interaction, a multiple linear regression approach was used given that both independent variables were continuous. We

predicted that if a rsFC × CST damage interaction was present, it would take the form of a stronger relationship between rsFC and behavior when CST damage was mild than when CST damage was severe. Establishing these relationships could have implications for the stratification and treatment of stroke patients during rehabilitation.

METHODS

Approach

Using diffusion tensor tractography (DTT), a template of the CST in healthy individuals was developed and used to calculate indices of CST damage in subacute stroke patients (< 4 weeks post stroke) with subcortical lesions. Along with stroke lesion volume these measures were correlated with a battery of motor scores. In parallel, BOLD fMRI measures of resting state functional connectivity (rsFC) were obtained in the somatomotor system and were correlated with CST damage and behavioral measures. Finally, the three-way relationship between CST damage, rsFC, and behavior was examined using multiple regression.

Participants

First time stroke patients were recruited. Potential candidates were identified by a research coordinator through daily monitoring of the inpatient service at Barnes-Jewish Hospital (BJH), and The Rehabilitation Institute of St. Louis (TRISL). Inclusion criteria were: a) age: over 18; b) four weeks or less since the time of infarct. Exclusion criteria were: a) prior strokes except for clinically silent lacunes, b) evidence of grade 3 periventricular white matter disease[36], c) dementia, defined as a score greater than 13 on the Short Blessed scale, d) medical conditions preventing survival for 12 months e) prior history of psychiatric conditions; however, patients with recent depression in the setting of stroke or minor depression in the past were enrolled.

Twenty-three patients (mean age 59.6 +/− 13 years (+/− s.d.), 12 women, 22 right-handed) participated in the study. All 23 patients underwent resting state fMRI scanning and 16 underwent motor testing. All subjects provided informed consent according to procedures established by the Washington University in Saint Louis Institutional Review Board and were compensated for their time. Thirteen healthy right-handed subjects participated in this study and were used to develop the CST template.

DTI Image acquisition in controls

In the healthy subjects imaging was performed on a 1.5 Tesla Siemens Vision scanner (Erlangen, Germany). Structural scans included a T1-weighted (T1W) sagittal magnetization-prepared rapid gradient echo (MPRAGE; TR=1900 ms, TI=1100 ms, TE=3.9 ms, flip angle 15°, 1×1×1.25-mm voxels) and a T2-weighted (T2W) fast spin echo scan (TR=4380 ms, TE = 94 ms, 1×1×3 mm). Diffusion weighted images were collected in 48 directions in a series of 4 acquisitions, each consisting of 12 directions using a locally modified echo planar imaging (EPI) sequence (TR=7000 ms, TE=113 ms, 2.5 isotropic voxels, b value = 800-1200 s/mm^2). Four complete DTI data sets were acquired in each participant.

DTI Registration

The first acquired, unsensitized (b = 0 s/mm^2) DTI volume was registered to the T2W image; stretch and shear was enabled (12 parameter affine transform) to partially compensate for EPI distortion. Atlas transformation was computed *via* the T1W image, which was registered to an atlas representative target produced by mutual co-registration of an MP-RAGE atlas produced from 12 normal, young adults[37].

Head motion correction

Each DTI volume dataset was motion corrected using three iterative cycles through a four step procedure (please see Supplementary Materials for details).

Region of Interest Identification for DTT

A superior ROI was placed in the posterior limb of the internal capsule (IC) at the level at which the superior-anterior fornix is oriented at a forty-five degree angle in the sagittal plane. Geniculate fibers of the posterior IC were excluded.

An inferior ROI was placed over the cerebral peduncle (CP). Tracing began three slices superior to the most superior slice on which the cerebro-pontine fibers are present. The cerebro-pontine fibers are easily and consistently identified on the RGB maps. Elliptical ROIs were drawn around the superior-inferior traveling fibers of the CP. An exclusionary ROI was traced around the CST in the pons to ensure that no fibers leaving the brainstem were included in the analysis.

DTT CST Template generation in controls

Whole brain streamline tractography[38,39] was performed for each subject by placing a seed point for tracking at every voxel in the subject's brain. Tracking was performed only in areas of anisotropy > 0.13 and a radius of curvature restriction of <1 mm was used as a stop criterion. Streamlines from a number of independent seedpoints could converge and traverse common voxels before diverging towards their endpoints. The streamline density in a particular voxel was therefore the number of streamline representations that traveled through that voxel.

The filtered CSTs were transformed to atlas space to construct a common CST template. CST maps were created by thresholding at ten percent of maximum streamline density. Individual subject binary maps were then summed to produce a composite map. This map was thresholded at a value of six (of thirteen) to produce a group model of the CST. The remaining analysis was performed with this template.

Quantification of CST Template Damage in Stroke Patients

Lesion segmentation was performed as previously reported.[16] The amount of CST template damage was quantified for each stroke patient by creating a conjunction map of the CST template with the lesion map for that individual. The total number of voxels at the intersection between each patient's stroke lesion map and the CST template was determined and was reported as a percentage of total CST template (% CST damage).

Resting State BOLD fMRI and Structural Scanning

Twenty-three acute stroke patients were scanned. A Siemens 3.0 Tesla Allegra MRI scanner was used. During resting-state BOLD fMRI scans, subjects were instructed to maintain fixation on a central cross projected onto a screen at the head of the magnet bore by a Sharp LCD projector ("Keep your eyes open, look at the cross"). Fixation and wakefulness were confirmed via infrared camera and no subject had to be excluded on this basis or due to excessive movement in the scanner. Participants viewed the stimuli through a mirror attached to the head coil. A gradient echo echo-planar sequence was used (TE = 25 ms, flip angle = 90°, 4×4×4 mm voxels, 32 contiguous slices, volume TR = 2.06 s) sensitive to BOLD contrast. Each BOLD fMRI scan (or run) consisted of 128 frames (or volumes) and lasted for 4.4 minutes. Six to eight resting scans were obtained for each subject, with a very brief break between each scan. The separate resting state BOLD fMRI runs for a subject were concatenated into a single data set for that subject. Structural images for atlas

transformation and lesion segmentation were acquired using a T1-weighted MP-RAGE (1×1×1.25 mm voxels; TE=3.93ms, TR=1810ms, TI=1200ms, flip angle=12 deg) and T2-weighted fast spin echo sequence (1.1×1.1×3.0 mm voxels; TE=96ms, TR=8430ms).

Atlas Transformations

An atlas representative MP-RAGE target was produced by mutual co-registration (12 parameter affine transformations) of images obtained in twelve normal subjects. Atlas transformation of the functional data was computed using the average of the first frame of each functional run and the T2 and MP-RAGE structural images. A cross-modal registration aligned the first frame average to the T2 image. A similar procedure registered the T2 image to the MP-RAGE image. An affine transformation then registered the MP-RAGE image to the atlas target. This target atlas was used for all the stroke patients. A separate representative MP-RAGE target was produced for the thirteen healthy subjects who contributed to the creation of the CST template using the same approach. This target was used for all the healthy subjects contributing to construction of the CST template.

Preprocessing of resting fMRI time-series

Preprocessing included compensation for asynchronous slice acquisition, elimination of odd even slice intensity differences resulting from interleaved acquisition, head motion compensation by six parameter rigid body realignment, whole brain intensity normalization, atlas transformation, spatial smoothing (6 mm FWHM Gaussian blur), temporal filtering retaining frequencies above .009 Hz and below 0.08 Hz, and removal by regression of several sources of variance unlikely to reflect spatially-specific functional correlations. The first 4 frames of each BOLD run were excluded from analysis because the net magnetization has not yet reached a steady state. Other details of preprocessing were the same as outlined by Fox et al.[40]

Definition of networks

Six core regions for the somatomotor network (central sulcus (CS), SMA, S2, putamen (Put), thalamus (Thal), contralateral cerebellum(CB)) were identified from the conjunction of significant voxels in two prior experiments in which healthy subjects pointed to stimuli on a screen with their right index finger, using only wrist rotation. A conjunction analysis indicated the right hand somatomotor network voxels that were present in five of the six motor seed maps. A left arm network was identified by flipping the six ROIs from across the midline and then repeating the same procedure.

ROI-to-ROI connectivity values

The average time course across voxels of one ROI was correlated with the average time course of other ROIs. Pearson correlation coefficients (r) for ROI pairs were calculated and the Fisher z transform was applied to yield measures that are approximately normally distributed. To compute an average connectivity score for multiple ROI pairs, the Fisher z-scores for the individual ROI pairs were averaged (see Supplementary Materials). These are the connectivity values that were used for all statistical analyses.

Voxel-wise functional connectivity maps from a single seed ROI (alex, this could be put in supplementary methods)

For purposes of illustration (Figure 5D), fcMRI maps corresponding to a selected seed ROI were generated. A BOLD time course was extracted from each voxel within the seed ROI and averaged across voxels. The average time course was then correlated with the timecourse of each voxel within the brain. The Fisher z transform was applied to the

correlation coefficient at each voxel and plotted to generate a functional connectivity map. Voxel-wise maps were not used for any statistical analysis.

Motor Testing

Active range of motion—Degrees of shoulder flexion, wrist flexion and wrist extension.[41]

Grip strength—A dynamometer measurement of the maximum amount of force produced during a five-finger grip.[42]

Action Research Arm Test (ARAT)—The ARAT measures upper extremity function using an ordinal score on 19 items (including tests of grasp, grip, pinch and gross motor function using a variety of objects). Maximum score is 57 indicating normal upper extremity function.[43] This test is highly sensitive to change at various time points post stroke and is well correlated with other upper extremity function measures.[44]

Nine Hole Peg Test (NHPT)—Subjects are timed in their ability to place 9 small pegs on a board and then remove them as quickly as possible.[45]

Functional Independence Measure – Walking Item—The FIM Walk is a lower-level measure of independent walking ability in patients with limited walking ability;[46] the score is an ordinal rating from 1 = complete dependence to 7 = independence.

Statistics

Statistical comparisons were performed in Predictive Analytics Soft Ware version 17 (previously SPSS, Chicago, Illinois). To study the relationship between CST damage and resting functional connectivity or behavior, bivariate correlations were calculated. To determine the amount of variance in behavioral scores that was attributable to CST damage or to changes in functional connectivity, multiple linear regression approach was used to investigate main effects. The % behavioral variance accounted for by any term was calculated as % Variance = (the Type III Sum of Squares for the term/ Type III Sum of Squares for the Corrected Total) * 100. To determine if there was a statistically significant interaction between rsFC and % CST damage on behavior, a separate multiple linear regression model was used containing the factors rsFC, % CST damage, and the interaction rsFC × % CST damage. This interaction was also studied using a 2-way ANOVA with median values defining the two levels for rsFC and for % CST damage (see Supplementary Materials).

RESULTS

Quantification of CST Damage after Stroke

Templates of the left and right CST were created based on DTT in 13 healthy individuals (Figure 1A). Each voxel included in a template was present in at least 6 out of 13 tractography maps.

Amount of CST damage was defined as the percentage of the total CST template volume that overlapped each stroke patient's lesion (% CST damage, Figure 1B), which were mainly subcortical (see Supplementary Table 1 for stroke subject characteristics) (Figure 1C). Mean CST damage was 16.02% (s.d. = +/− 3.42). No subject had evidence of old CST lacunes.

Effect of CST Damage on Resting Connectivity

CST damage was significantly correlated with inter-hemispheric connectivity (Pearson r = −0.592, p = 0.004) (Figure 2, left panel) and ipsilesional intra-hemispheric connectivity (Pearson r = −0.537, p = 0.01) (middle panel), but not with contralesional intra-hemispheric connectivity (Pearson r = 0.056, p = 0.8) (right panel). However, % CST damage was significantly correlated with lesion volume (Pearson r = 0.659, p<0.001). Following a partial correlation analysis to control for the effect of lesion size, CST damage was still significantly correlated with inter-hemispheric connectivity (partial r = −0.433, p = 0.05) but not with ipsilesional intra-hemispheric connectivity or contralesional intra-hemispheric connectivity (partial r = −0.252, p = 0.27; partial r = −0.033, p = 0.89, respectively).

Correlations between % CST damage and inter-hemispheric connectivity were also investigated for 6 homotopic ROI pairs in our somatomotor network (central sulcus (CS), secondary somatosensory region (S2), supplementary motor area (SMA), putamen (Put), thalamus (Thal) and cerebellum (CB)). Three subjects with more than 50% damage to any motor ROI were excluded. Percent CST damage was significantly correlated with changes in rsFC between left and right CS containing primary motor cortex (Pearson r = −0.623, p = 0.004). This relationship was not caused by structural damage as the lesion distribution did not overlap with the CS.[16] No significant correlation was observed between % CST damage and inter-hemispheric rsFC for the other ROIs or between % CST damage and connectivity between the ipsilesional CS and other ipsilesional somatomotor ROIs.

Contributions of Resting State Functional Connectivity and CST Damage to Motor Impairment

We found a strong correlation between motor impairment and % CST damage but not stroke lesion size (Figure 3). Because % CST damage influences the strength of inter-hemispheric rsFC (see previous section), it is important to disentangle the relative importance of % CST damage and inter-hemispheric connectivity on motor behavior, and determine whether they have independent effects or interact with each other. We first performed a multiple linear regression to examine the main effects of % CST damage and rsFC on motor behavior. For 5 of the 7 behaviors tested, % CST damage accounted for a significant percentage of the variance in motor performance (Figure 4). Inter-hemispheric rsFC did not account for a significant amount of variance in this model. A second analysis that added stroke lesion size and *intra-hemispheric* rsFC to the linear regression model resulted in significant regression coefficients for % CST damage in all motor tests. No other factor was significant except for Grip Strength, where stroke lesion size ((F 1,10) = 6.6, p = 0.028) explained 18.2% of the variance in performance (see Supplementary Table 2). Overall, the results were similar to our original analysis and did not result in a change in interpretation.

The lack of relationship between inter-hemispheric rsFC and behavior in the above analyses may seem inconsistent with our previous report of a correlation between inter-hemispheric connectivity and behavior. However, effects of inter-hemispheric rsFC may depend on the amount of CST damage. Specifically, substantial CST damage may reduce or eliminate the relationship between inter-hemispheric connectivity and behavior. To investigate this possibility, a separate linear regression model was computed with the factors inter-hemispheric rsFC, % CST damage and inter-hemispheric rsFC × % CST damage. Because our initial analyses showed no correlation between stroke lesion size and motor performance (Figure 3) stroke lesion size was not included in this model. We found that the interaction term accounted for a significant portion of the variance in performance for Grip Strength (% variance = 26.82, p = 0.01), NHPT (% variance = 25.03, p = 0.014), Shoulder Flexion (% variance = 13.58, p = 0.042), Wrist Flexion (% variance = 13.77, p = 0.05), a marginal

portion of the variance for the ARAT (% variance = 10.65, p = 0.084), and no significant portion for Wrist Extension or the FIM Walk (Figure 4; Supplementary Table 3).

The nature of this interaction is qualitatively illustrated in Figures 5A and 5B, which shows the relationship between motor performance and CST damage (5A) or rsFC (5B). Motor performance drops off quickly with increasing CST damage (red and white circles, Figure 5A), reaching a floor with high levels of CST damage (black circles, 5A). Correspondingly, motor performance increases with increasing rsFC for patients with low CST damage (red and white circles, Figure 5B), but remains impaired for patients with high damage even as rsFC increases (black circles, Figure 5B). The 5 subjects who had the greatest %CST damage showed poor performance across all motor tasks regardless of varying levels of inter-hemispheric rsFC (Figure 5B). These results suggest that when CST damage is low, motor function is correlated with inter-hemispheric rsFC, but that when CST damage exceeds a certain level, rsFC no longer affects the degree of impairment.

This conclusion was supported by a two-way ANOVA in which median values for inter-hemispheric rsFC (0.594) and % CST damage (10.188) served as cut-offs for defining low and high levels of the rsFC and % CST damage factors. A significant main effect of % CST damage was observed in 6 of 7 tasks. A significant main effect of inter-hemispheric rsFC and a significant rsFC × % CST Damage interaction ((F 1,10) = 8.53, p = 0.015) was detected for Grip Strength (see Supplementary Table 4 for details). Grip Strength was not dependent on inter-hemispheric rsFC when CST damage was severe but was dependent on inter-hemispheric rsFC when CST damage was mild (see Supplementary Figure 1). Scatter plots of the behavioral-rsFC relationship for subjects belonging to the two levels of % CST damage (Figure 6) were consistent with the above conclusion.

Discussion

Our results show that structural damage to the CST, as determined by a template derived from diffusion tensor imaging in healthy controls, was associated with decreased somatomotor inter-hemispheric rsFC. These rsFC changes reflect a physiological impairment of spontaneous activity coherence upstream from the site of damage. Secondly, rsFC was significantly related to motor performance only when CST damage was less than about 10% of the total volume of the CST template. Hence post-stroke motor deficits reflect a complex interaction of structural and functional impairments in brain motor networks.

Upstream Functional Consequences of CST Damage

The correlation between decreased interhemispheric rsFC and increasing CST damage was strongest for rsFC between left and right sensory-motor cortex. It was not dependent on overall stroke volume or interruption of fibers to/from primary sensory-motor cortex within the damaged hemisphere, since no correlation was observed between CST damage and rsFC between ROIs within the damaged hemisphere. Damage to transcallosal motor fibers also cannot explain the effect, as the lesion distribution in our sample was located more anterior, inferior and medial[47,48].

Timecourse of Retrograde Changes after CST Damage

Our results suggest that disruption of rsFC is a remote upstream effect of CST damage on cortical structures. Wallerian degeneration in the pyramidal tract after stroke has been reported within 2 weeks with DTI. [49-51,52] The extent and time course of retrograde degeneration in the proximal portion of the corticospinal tract are less well understood. Animal evidence exists for early retrograde changes in pyramidal layer V[53]. Longitudinal DTI studies of retrograde pyramidal degeneration after spinal cord,[54] pontine,[55] or

subcortical lesions[56] all show a similar pattern with degeneration in the corticospinal tract slowly marching more rostrally. However, there is no conclusive evidence of changes in FA in the centrum semiovale or corona radiata before 1 month after CST damage. Therefore, it seems unlikely that extensive retrograde degeneration can explain the changes in network functional connectivity observed in our subacute stroke population.

Functional Network Reorganization after Infarct

CST damage can lead to functional changes in cortical responses, including increased movement-related BOLD activations[57,58] and recruitment of supplementary motor areas as well as ipsilesional and contralesional M1/S1 regions[59]. These results are consistent with prior studies showing recruitment of secondary motor and contralesional areas, as well as larger activations in these same areas in patients with more severe strokes and greater disruption of CST integrity [60-62]. CST damage can also affect spontaneous cortical activity, consistent with the present results. In a recent longitudinal study of subcortical stroke, Wang et al[63] reported that motor cortical reorganization and recovery are associated with a loss of regional node importance, decreased inter-hemispheric rsFC between subcortical ROIs and increased inter-hemispheric rsFC between cortical ROIs. In recent animal experiments, Van Meer and colleagues found a significant correlation of rsFC between left and right primary motor cortex with motor behavior in rats with subcortical lesions[17].

Behavioral Relevance of Connectivity Varies with Context

Network-specific coherent spontaneous BOLD fluctuations explain a significant portion of the variability in BOLD responses,[64] reaction times and button press force,[65] and are correlated with hemispatial neglect[14] and with motor function.[16] Here we show that the behavioral significance of rsFC varies with the degree of CST damage. For CST damage equal to less than **approximately 10%** we found a significant correlation between motor impairment and functional connectivity. However, when CST damage is greater, motor deficits are driven primarily by the CST damage although cortical functional connectivity may be quite abnormal as well.

In our linear regression analysis, the rsFC × % CST damage interaction was significant in 4 of the 7 behavioral tests and was marginal in another. The interaction was significant in the 2-way ANOVA for only 1 test, but the ANOVA has reduced sensitivity relative to the regression analyses since it requires that continuous independent variables be categorized. Bebee et al showed that six standardized tests of upper extremity function were highly correlated with each other and loaded onto a single factor.[66] However, whether different motor tests focus on separate dimensions of motor performance or rely on brain regions with different contributions to the CST was beyond the scope of the present study.

CST Damage and Motor Recovery

Very recently, Zhu et al reported that CST lesion load was highly correlated with upper extremity Fugl-Meyer scores[26]. Our findings are consistent with the results of these and other previous studies demonstrating a robust association between CST damage assessed by DTI and motor impairment in stroke[25,67-74]. However, Sterr et al, recently reported that even subjects with severe CST damage showed behavioral gains after constraint-induced movement therapy.[27] Other measures such as the presence of motor evoked potentials elicited by transcranial magnetic stimulation may provide additional useful information about the state of the motor network[25,75] and its potential for further recovery. Our results, which show that inter-hemispheric rsFC is disrupted after CST damage, suggest that both the focal lesion and its remote effects on network function are relevant to understanding recovery after stroke.

Supplementary Material

Refer to Web version on PubMed Central for supplementary material.

Acknowledgments

This study was supported by the National Institute of Mental Health [R01 HD061117-05A2 to M.C.; 1K08NS064365-01A1 to A.R.C.], the Robert Wood Johnson Foundation Amos Medical Faculty Development Program [65592 to A.R.C.], and the Rehabilitation Institute of St. Louis. We thank Adrian Epstein for his guidance with regard to the analysis of the diffusion tensor imaging data.

References

1. Honey CJ, Sporns O. Dynamical consequences of lesions in cortical networks. Hum Brain Mapp. 2008; 29:802–9. [PubMed: 18438885]
2. Watts DJ, Strogatz SH. Collective dynamics of small-world networks. Nature. 1998; 393:440–42. [PubMed: 9623998]
3. Friston KJ, Dolan RJ. Computational and dynamic models in neuroimaging. Neuroimage. 2010; 52:752–65. [PubMed: 20036335]
4. Tononi G, Sporns O, Edelman GM. A measure for brain complexity: relating functional segregation and integration in the nervous system. Proc Natl Acad Sci USA. 1994; 91:5033–7. [PubMed: 8197179]
5. Friston KJ. Modalities, modes, and models in functional neuroimaging. Science. 2009; 326:399–403. [PubMed: 19833961]
6. Ward NS, Brown MM, Thompson AJ, Frackowiak RS. Neural correlates of motor recovery after stroke: a longitudinal fMRI study. Brain. 2003; 126:2476–96. [PubMed: 12937084]
7. Ward NS, Brown MM, Thompson AJ, Frackowiak RS. Neural correlates of outcome after stroke: a cross-sectional fMRI study. Brain. 2003; 126:1430–48. [PubMed: 12764063]
8. Corbetta M, Kincade MJ, Lewis C, Snyder AZ, Sapir A. Neural basis and recovery of spatial attention deficits in spatial neglect. Nat Neurosci. 2005; 8:1603–10. [PubMed: 16234807]
9. Saur D, Lange R, Baumgaertner A, et al. Dynamics of language reorganization after stroke. Brain. 2006; 129:1371–84. [PubMed: 16638796]
10. Calautti C, Naccarato M, Jones PS, et al. The relationship between motor deficit and hemisphere activation balance after stroke: A 3T fMRI study. Neuroimage. 2007; 34:322–31. [PubMed: 17045490]
11. Sharma N, Baron JC, Rowe JB. Motor imagery after stroke: relating outcome to motor network connectivity. Ann Neurol. 2009; 66:604–16. [PubMed: 19938103]
12. Cramer SC. Repairing the human brain after stroke: I. Mechanisms of spontaneous recovery. Ann Neurol. 2008; 63:272–87. [PubMed: 18383072]
13. Calautti C, Jones PS, Naccarato M, et al. The relationship between motor deficit and primary motor cortex hemispheric activation balance after stroke: longitudinal fMRI study. J Neurol Neurosurg Psychiatry. 2010; 81:788–92. [PubMed: 20392975]
14. He BJ, Snyder AZ, Vincent JL, Epstein A, Shulman GL, Corbetta M. Breakdown of functional connectivity in frontoparietal networks underlies behavioral deficits in spatial neglect. Neuron. 2007; 53:905–18. [PubMed: 17359924]
15. Grefkes C, Nowak DA, Eickhoff SB, et al. Cortical connectivity after subcortical stroke assessed with functional magnetic resonance imaging. Ann Neurol. 2008; 63:236–46. [PubMed: 17896791]
16. Carter AR, Astafiev SV, Lang CE, et al. Resting inter-hemispheric functional magnetic resonance imaging connectivity predicts performance after stroke. Ann Neurol. 2010; 67:365–75. [PubMed: 20373348]
17. van Meer MP, van der Marel K, Wang K, et al. Recovery of sensorimotor function after experimental stroke correlates with restoration of resting-state inter-hemispheric functional connectivity. J Neurosci. 2010; 30:3964–72. [PubMed: 20237267]

18. von Monakow C. Lokalisation der Hirnfunktionen [Localization of brain functions]. Journal fur Psychologie and Neurologie. 1911; 17:185–200.
19. Finger S, Koehler PJ, Jagella C. The Monakow concept of diaschisis: origins and perspectives. Arch Neurol. 2004; 61:283–8. [PubMed: 14967781]
20. Biswal B, Yetkin F, Haughton V, Hyde J. Functional connectivity in the motor cortex of resting human brain using echo-planar MRI. Magnetic Resonance in Medicine. 1995; 34:537–41. [PubMed: 8524021]
21. Katz PS. Neurons, networks, and motor behavior. Neuron. 1996; 16:245–53. [PubMed: 8789940]
22. Schieber MH. Chapter 2 Comparative anatomy and physiology of the corticospinal system. Handb Clin Neurol. 2007; 82:15–37. [PubMed: 18808887]
23. Shadmehr R, Krakauer JW. A computational neuroanatomy for motor control. Exp Brain Res. 2008; 185:359–81. [PubMed: 18251019]
24. Lemon RN. Descending pathways in motor control. Annu Rev Neurosci. 2008; 31:195–218. [PubMed: 18558853]
25. Stinear CM, Barber PA, Smale PR, Coxon JP, Fleming MK, Byblow WD. Functional potential in chronic stroke patients depends on corticospinal tract integrity. Brain. 2007; 130:170–80. [PubMed: 17148468]
26. Zhu LL, Lindenberg R, Alexander MP, Schlaug G. Lesion Load of the Corticospinal Tract Predicts Motor Impairment in Chronic Stroke. Stroke. 2010; 41:910–5. [PubMed: 20378864]
27. Sterr A, Shen S, Szameitat AJ, Herron KA. The role of corticospinal tract damage in chronic motor recovery and neurorehabilitation: a pilot study. Neurorehabil Neural Repair. 2010; 24:413–9. [PubMed: 20516488]
28. Zhang D, Snyder AZ, Fox MD, Sansbury MW, Shimony JS, Raichle ME. Intrinsic functional relations between human cerebral cortex and thalamus. J Neurophysiol. 2008; 100:1740–8. [PubMed: 18701759]
29. Habas C. Functional connectivity of the human rostral and caudal cingulate motor areas in the brain resting state at 3T. Neuroradiology. 2010; 52:47–59. [PubMed: 19629462]
30. Ward NS. Neural plasticity and recovery of function. Prog Brain Res. 2005; 150:527–35. [PubMed: 16186046]
31. Kokotilo KJ, Eng JJ, Boyd LA. Reorganization of brain function during force production after stroke: a systematic review of the literature. J Neurol Phys Ther. 2009; 33:45–54. [PubMed: 19265770]
32. Lewis, CCM.; Committeri, G.; Romani, G.; Baldassare, A. Perceptual learning modulates resting state functional connectivity between visual cortex and dorsal attention network. Society for Neuroscience; Washington, D.C.: 2008.
33. Albert NB, Robertson EM, Miall RC. The resting human brain and motor learning. Curr Biol. 2009; 19:1023–7. [PubMed: 19427210]
34. Tambini A, Ketz N, Davachi L. Enhanced brain correlations during rest are related to memory for recent experiences. Neuron. 2010; 65:280–90. [PubMed: 20152133]
35. Liu Z, Li Y, Zhang X, Savant-Bhonsale S, Chopp M. Contralesional axonal remodeling of the corticospinal system in adult rats after stroke and bone marrow stromal cell treatment. Stroke. 2008; 39:2571–7. [PubMed: 18617661]
36. de Groot JC, de Leeuw FE, Oudkerk M, et al. Cerebral white matter lesions and cognitive function: the Rotterdam Scan Study. Ann Neurol. 2000; 47:145–51. [PubMed: 10665484]
37. Shimony JS, Burton H, Epstein AA, McLaren DG, Sun SW, Snyder AZ. Diffusion tensor imaging reveals white matter reorganization in early blind humans. Cereb Cortex. 2006; 16:1653–61. [PubMed: 16400157]
38. Mori S, Crain BJ, Chacko VP, van Zijl PC. Three-dimensional tracking of axonal projections in the brain by magnetic resonance imaging. Ann Neurol. 1999; 45:265–9. [PubMed: 9989633]
39. Conturo TE, Lori NF, Cull TS, et al. Tracking neuronal fiber pathways in the living human brain. Proc Natl Acad Sci USA. 1999; 96:10422–27. [PubMed: 10468624]

40. Fox MD, Snyder AZ, Vincent JL, Corbetta M, Van Essen DC, Raichle ME. The human brain is intrinsically organized into dynamic, anticorrelated functional networks. Proc Natl Acad Sci U S A. 2005; 102:9673–8. [PubMed: 15976020]
41. Gajdosik RL, Bohannon RW. Clinical measurement of range of motion. Review of goniometry emphasizing reliability and validity. Phys Ther. 1987; 67:1867–72. [PubMed: 3685114]
42. Schmidt RT, Toews JV. Grip strength as measured by the Jamar dynamometer. Arch Phys Med Rehabil. 1970; 51:321–7. [PubMed: 5423802]
43. Lyle RC. A performance test for assessment of upper limb function in physical rehabilitation treatment and research. Int J Rehabil Res. 1981; 4:483–92. [PubMed: 7333761]
44. Hsieh CL, Hsueh IP, Chiang FM, Lin PH. Inter-rater reliability and validity of the action research arm test in stroke patients. Age Ageing. 1998; 27:107–13. [PubMed: 16296669]
45. Wade DT. Measuring arm impairment and disability after stroke. Int Disabil Stud. 1989; 11:89–92. [PubMed: 2698395]
46. Simondson JA, Goldie P, Greenwood KM. The Mobility Scale for Acute Stroke Patients: concurrent validity. Clin Rehabil. 2003; 17:558–64. [PubMed: 12952164]
47. Hofer S, Frahm J. Topography of the human corpus callosum revisited--comprehensive fiber tractography using diffusion tensor magnetic resonance imaging. Neuroimage. 2006; 32:989–94. [PubMed: 16854598]
48. Wahl M, Lauterbach-Soon B, Hattingen E, et al. Human motor corpus callosum: topography, somatotopy, and link between microstructure and function. J Neurosci. 2007; 27:12132–8. [PubMed: 17989279]
49. Stovring J, Fernando LT. Wallerian degeneration of the corticospinal tract region of the brain stem: demonstration by computed tomography. Radiology. 1983; 149:717–20. [PubMed: 6647849]
50. Thomalla G, Glauche V, Koch MA, Beaulieu C, Weiller C, Rother J. Diffusion tensor imaging detects early Wallerian degeneration of the pyramidal tract after ischemic stroke. Neuroimage. 2004; 22:1767–74. [PubMed: 15275932]
51. Thomalla G, Glauche V, Weiller C, Rother J. Time course of wallerian degeneration after ischaemic stroke revealed by diffusion tensor imaging. J Neurol Neurosurg Psychiatry. 2005; 76:266–8. [PubMed: 15654048]
52. Puig J, Pedraza S, Blasco G, et al. Wallerian degeneration in the corticospinal tract evaluated by diffusion tensor imaging correlates with motor deficit 30 days after middle cerebral artery ischemic stroke. AJNR Am J Neuroradiol. 2010; 31:1324–30. [PubMed: 20299434]
53. Kalil K, Schneider GE. Retrograde cortical aand axonal changes following lesions of the pyramidal tract. Brain Res. 1975; 89:15–27. [PubMed: 1148840]
54. Guleria S, Gupta RK, Saksena S, et al. Retrograde Wallerian degeneration of cranial corticospinal tracts in cervical spinal cord injury patients using diffusion tensor imaging. J Neurosci Res. 2008; 86:2271–80. [PubMed: 18335542]
55. Liang Z, Zeng J, Zhang C, et al. Longitudinal investigations on the anterograde and retrograde degeneration in the pyramidal tract following pontine infarction with diffusion tensor imaging. Cerebrovasc Dis. 2008; 25:209–16. [PubMed: 18216462]
56. Liang Z, Zeng J, Liu S, et al. A prospective study of secondary degeneration following subcortical infarction using diffusion tensor imaging. J Neurol Neurosurg Psychiatry. 2007; 78:581–6. [PubMed: 17237143]
57. Hamzei F, Dettmers C, Rijntjes M, Weiller C. The effect of cortico-spinal tract damage on primary sensorimotor cortex activation after rehabilitation therapy. Exp Brain Res. 2008; 190:329–36. [PubMed: 18592223]
58. Schaechter JD, Perdue KL. Enhanced cortical activation in the contralesional hemisphere of chronic stroke patients in response to motor skill challenge. Cereb Cortex. 2008; 18:638–47. [PubMed: 17602141]
59. Schaechter JD, Perdue KL, Wang R. Structural damage to the corticospinal tract correlates with bilateral sensorimotor cortex reorganization in stroke patients. Neuroimage. 2008; 39:1370–82. [PubMed: 18024157]

60. Gerloff C, Bushara K, Sailer A, et al. Multimodal imaging of brain reorganization in motor areas of the contralesional hemisphere of well recovered patients after capsular stroke. Brain. 2006; 129:791–808. [PubMed: 16364955]
61. Ward NS, Newton JM, Swayne OB, et al. Motor system activation after subcortical stroke depends on corticospinal system integrity. Brain. 2006; 129:809–19. [PubMed: 16421171]
62. Ward NS, Newton JM, Swayne OB, et al. The relationship between brain activity and peak grip force is modulated by corticospinal system integrity after subcortical stroke. Eur J Neurosci. 2007; 25:1865–73. [PubMed: 17432972]
63. Wang L, Yu C, Chen H, et al. Dynamic functional reorganization of the motor execution network after stroke. Brain. 2010; 133:1224–38. [PubMed: 20354002]
64. Fox MD, Snyder AZ, Zacks JM, Raichle ME. Coherent spontaneous activity accounts for trial-to-trial variability in human evoked brain responses. Nat Neurosci. 2006; 9:23–5. [PubMed: 16341210]
65. Fox MD, Snyder AZ, Vincent JL, Raichle ME. Intrinsic fluctuations within cortical systems account for intertrial variability in human behavior. Neuron. 2007; 56:171–84. [PubMed: 17920023]
66. Beebe JA, Lang CE. Relationships and responsiveness of six upper extremity function tests during the first six months of recovery after stroke. J Neurol Phys Ther. 2009; 33:96–103. [PubMed: 19556918]
67. Pineiro R, Pendlebury ST, Smith S, et al. Relating MRI changes to motor deficit after ischemic stroke by segmentation of functional motor pathways. Stroke. 2000; 31:672–9. [PubMed: 10700503]
68. Watanabe T, Honda Y, Fujii Y, Koyama M, Matsuzawa H, Tanaka R. Three-dimensional anisotropy contrast magnetic resonance axonography to predict the prognosis for motor function in patients suffering from stroke. J Neurosurg. 2001; 94:955–60. [PubMed: 11409525]
69. Lee JS, Han MK, Kim SH, Kwon OK, Kim JH. Fiber tracking by diffusion tensor imaging in corticospinal tract stroke: Topographical correlation with clinical symptoms. Neuroimage. 2005; 26:771–6. [PubMed: 15955486]
70. Cho SH, Kim DG, Kim DS, Kim YH, Lee CH, Jang SH. Motor outcome according to the integrity of the corticospinal tract determined by diffusion tensor tractography in the early stage of corona radiata infarct. Neurosci Lett. 2007; 426:123–7. [PubMed: 17897782]
71. Jang SH, Bai D, Son SM, et al. Motor outcome prediction using diffusion tensor tractography in pontine infarct. Ann Neurol. 2008; 64:460–5. [PubMed: 18661560]
72. Schaechter JD, Fricker ZP, Perdue KL, et al. Microstructural status of ipsilesional and contralesional corticospinal tract correlates with motor skill in chronic stroke patients. Hum Brain Mapp. 2009; 30:3461–74. [PubMed: 19370766]
73. Kusano Y, Seguchi T, Horiuchi T, et al. Prediction of functional outcome in acute cerebral hemorrhage using diffusion tensor imaging at 3T: a prospective study. AJNR Am J Neuroradiol. 2009; 30:1561–5. [PubMed: 19556354]
74. Lindenberg R, Renga V, Zhu LL, Betzler F, Alsop D, Schlaug G. Structural integrity of corticospinal motor fibers predicts motor impairment in chronic stroke. Neurology. 2010; 74:280–7. [PubMed: 20101033]
75. Perez MA, Cohen LG. The corticospinal system and transcranial magnetic stimulation in stroke. Top Stroke Rehabil. 2009; 16:254–69. [PubMed: 19740731]

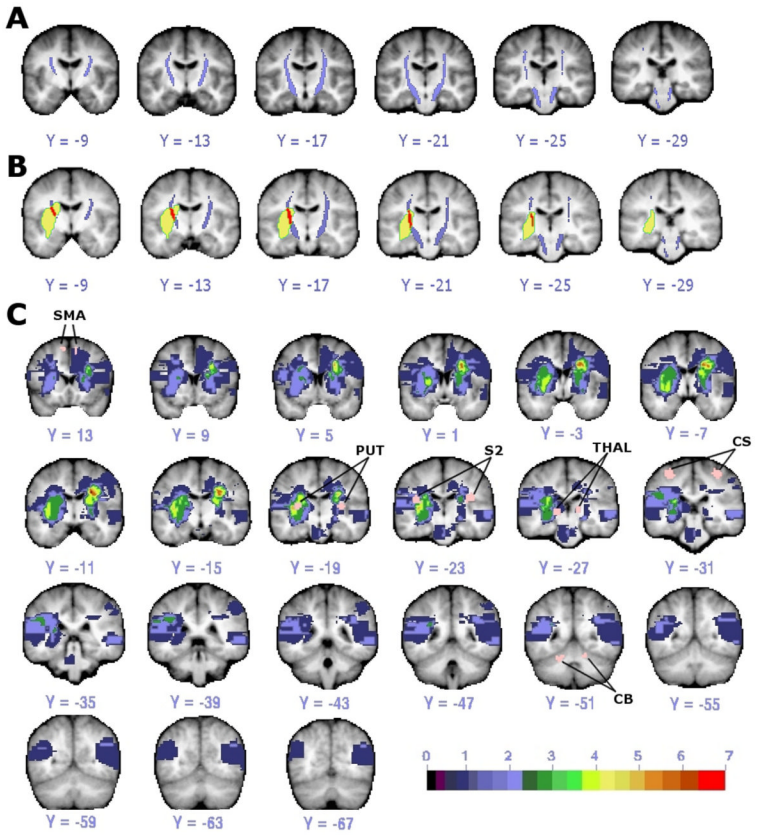

Figure 1. DTI template of CST and lesion distribution

(A) CST template (purple) from healthy individuals with threshold of 6 of 13 subjects is shown. (B) Overlap (red) of CST template (purple) and lesion (yellow) in one stroke subject. (C) Lesion distribution in 22 stroke patients with ROIs used as seeds in functional connectivity analysis colored in pink and labeled. Color scale indicates number of subjects with lesion at that voxel. (Small areas of diffusion restriction could not be quantified in one subject.) CS: central sulcus; SMA: supplementary motor area; PUT: putamen; THAL: thalamus; S2: secondary somatosensory area; CB: cerebellum.

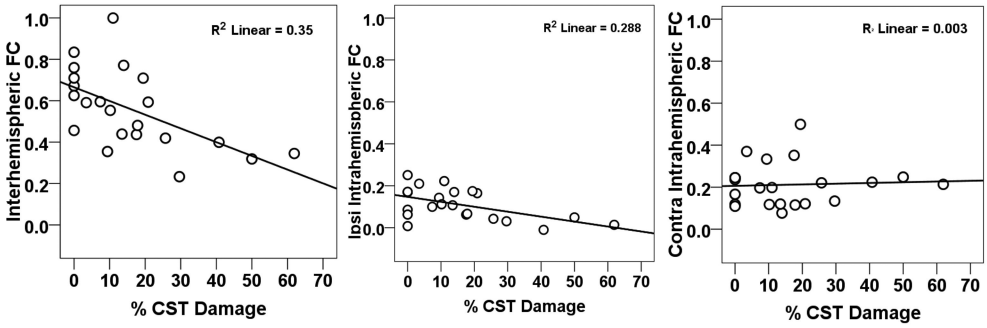

Figure 2. Scatter plots of resting connectivity as a function of % CST damage

Ipsi = ipsilesional; contra = contralesional; fcMRI = functional connectivity; % CST = % corticospinal tract damage.

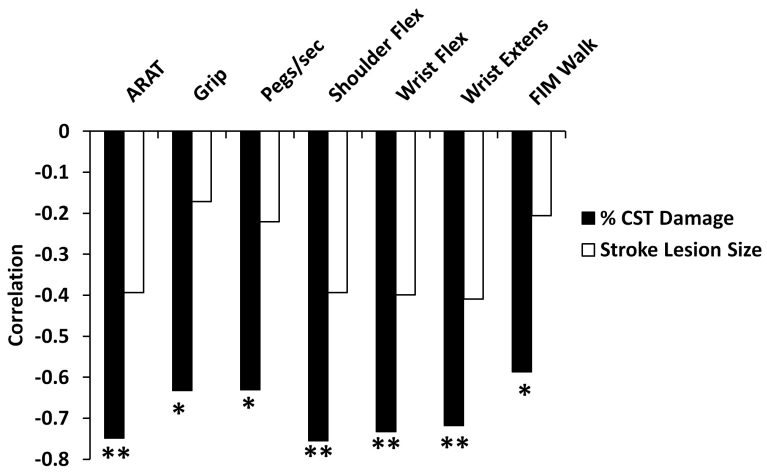

Figure 3. Correlation of % CST damage with measures of motor function

CST = corticospinal track; ARAT = Action Research Arm Test; Flex = flexion; Extens = extension; FIM = Functional Independence Measure; * $p < 0.05$; ** $p < 0.01$.

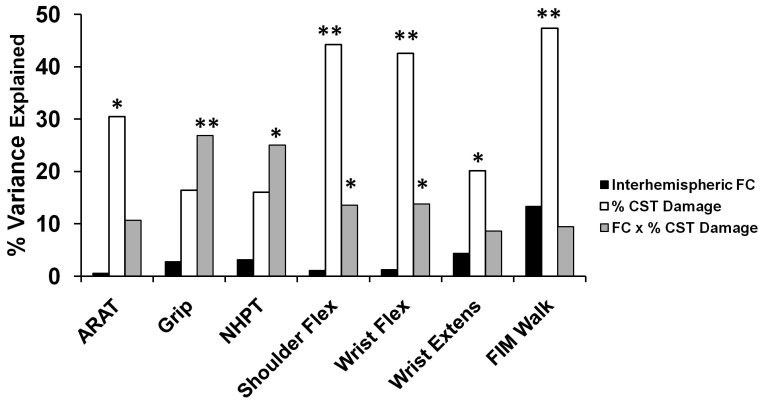

Figure 4. Linear regression analysis to determine the % variance in performance accounted for by amount of CST damage, inter-hemispheric fcMRI, and the CST damage × inter-hemispheric rsFC interaction

ARAT = Action Research Arm Test; Flex = flexion; Extens = extension; FIM = Functional Independence Measure; FC = functional connectivity; CST = corticospinal track; * = $p < 0.05$; ** = $p < 0.01$

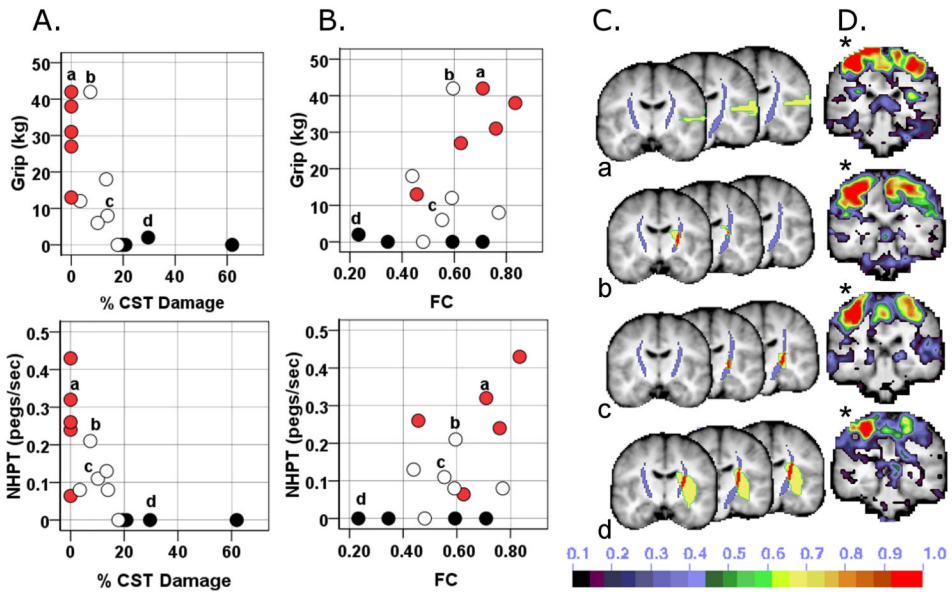

Figure 5. Dual contribution of CST damage and impaired inter-hemispheric rsFC to motor impairment

A) Scatter plots relating motor performace and % CST damage. B) Scatter plots relating motor performance and rsFC. Blackened circles = 75th percentile for CST damage; white circles = 25th to 74th percentile; red circles = no CST damage. C) Intersection (red) of CST template (purple) with stroke lesion (yellow) for 4 individuals labeled a,b,c,d. D) Seed-based functional connectivity map for the same 4 individuals when seeding the contralesional undamaged central sulcus (*). NHPT: nine whole peg test; FC: functional connectivity; CS: central sulcus; % CST: % corticospinal tract damaged.

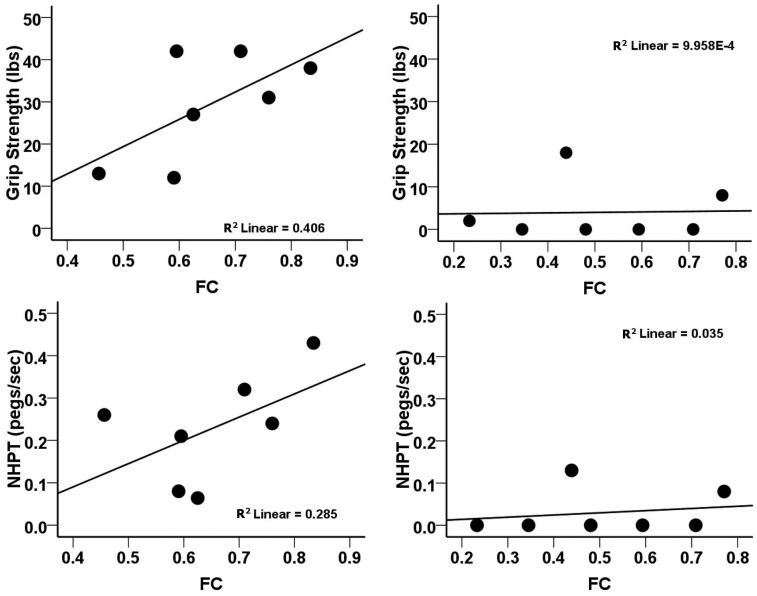

Figure 6. Effect of impaired inter-hemispheric rsFC on motor impairment depends on the extent of CST damage

A) Scatter plots relating motor performace and inter-hemispheric rsFC in subgroup of subjects with % CST damage below the median for the distribution of % CST values. B) Scatter plots relating motor performace and inter-hemispheric rsFC in subgroup of subjects with % CST damage above the median for the distribution of % CST values. NHPT: nine whole peg test; FC: inter-hemispheric resting state functional connectivity.